Joint Source-Channel Coding and Power Adaptation for Energy Efficient Wireless Video Communications

Fan Zhai, Yiftach Eisenberg, Thrasyvoulos N. Pappas,

Randall Berry, and Aggelos K. Katsaggelos*

Department of Electrical and Computer Engineering

Northwestern University

2145 Sheridan Road, Evanston, IL 60208, USA

Email: {fzhai, yeisenbe, pappas, rberry, aggk}@ece.northwestern.edu

*Correspondence: Prof. Aggelos K. Katsaggelos

Department of Electrical and Computer Engineering

Northwestern University

2145 Sheridan Road, Evanston, IL 60208, USA

Phone: (847) 491-7146

Fax: (847) 491-4455

Email: aggk@ece.northwestern.edu

Abstract

We consider efficiently transmitting video over a hybrid wireless/wire-line network by optimally allocating resources across multiple protocol layers. Specifically, we present a framework of joint source-channel coding and power adaptation, where error resilient source coding, channel coding, and transmission power adaptation are jointly designed to optimize video quality given constraints on the total transmission energy and delay for each video frame. In particular, we consider the combination of two types of channel coding - inter-packet coding (at the transport layer) to provide protection against packet dropping in the wire-line network and intra-packet coding (at the link layer) to provide protection against bit errors in the wireless link. In both cases, we allow the coding rate to be adaptive to provide unequal error protection at both the packet and frame level. In addition to both types of channel coding, we also compensate for channel errors by adapting the transmission power used to send each packet. An efficient algorithm based on Lagrangian relaxation and the method of alternating variables is proposed to solve the resulting optimization problem. Simulation results are shown to illustrate the advantages of joint optimization across multiple layers.

Keywords

I. INTRODUCTION

Real-time network-based video applications, such as videoconferencing, distance learning and on-demand video streaming, have gained increased popularity. In addition, developing wireless technologies, such as the third generation (3G) and fourth generation (4G) cellular systems, IEEE 802.11, and Bluetooth systems, are expanding the scope of existing video applications and leading to the creation of new ones such as multimedia messaging services (MMS). Real-time video transmission over networks that contain such wireless links, however, is still a challenging problem, due to the limited and time-varying channel bandwidth. Also, most of these emerging wireless technologies use an IP (Internet Protocol) based architecture; whereas it is well known that the best effort design of the current IP protocols makes it difficult to provide the quality of service (QoS) needed by real-time video applications. A direct approach dealing with the lack of QoS is to use error control. In addition, in order to efficiently utilize the limited network resources such as bandwidth and battery energy, the video transmission end system should be network adaptive. An essential method to achieve both of these is through cross-layer design [3].

Cross-layer design of multimedia transmission aims to improve the overall system's performance by jointly considering multiple protocol layers. For real-time video applications, cross-layer design may involve the video encoder and all the underlying network layers. The encoder can adjust its behavior, e.g., its flow rate or the amount of overhead devoted to error resilience, by selecting the source coding parameter for each video packet based on the changing network conditions. This technique is usually referred to as *error resilient source coding*. The adaptation can also take place in the underlying layers, such as the application layer and transport layer, e.g., by adding redundancy for forward error correction (FEC) or employing Automatic Repeat reQurest (ARQ) to retransmit lost packets [4]. For wireless networks, FEC and ARQ can also operate in the link layer [5]. In the physical layer, there are yet more adaptation tools, such as FEC, modulation modes, power control, and transmission rate adaptation [6]. To increase resource utilization efficiency, those adaptations should be performed according to the information derived from the application such as QoS priorities, as well as the available channel state information (CSI).

Cross-layer design for video applications is a broad area of research and development. Generally speaking, it can be classified into two major approaches. One approach is to focus on developing new network protocols and mechanisms to adapt the network to the video applications. Examples of this include developing new transport layer protocols for multimedia streaming as in [7] or approaches that modify the mechanisms implemented in the routers and switches to provide QoS support for video applications (such as the differentiated service architecture [8]). This type of work is beyond the scope of this paper. The second type of approach is to adapt the streaming end system (across multiple protocol layers) to the rest of the network, which is what we employ here. To be more precise, we assume that the lower layer provides a set of given adaptation components; from the encoder's point of view these components can be regarded as network resource allocation "knobs". Our goal is to specify how the end-system should use these components to jointly allocate resources.

Different lower layer adaptation components may be able to be combined into one type of resource allocation "knob". For example, although physical layer FEC, modulation

modes, power adaptation, and transmission rate adaptation are different techniques, from the encoder's point of view, all that matters is the resulting performance in terms of packet loss probability, energy consumption and data rate, not the exact combination of techniques used to achieve this. We assume that the encoder can access and specify a set of lower layer resource allocation parameters. Then the question is how to optimally allocate the available network resources to achieve the best video quality. Since video packets are usually of different importance, the network resources should be allocated to packets according to their importance in order to provide optimal unequal error protection (UEP). To achieve this, we propose a resource-distortion optimization framework for jointly allocating the given resources. Specifically, at the sender side, we consider error resilient source coding at the encoder, transport-layer FEC, link-layer FEC, and power adaptation at the physical layer. When evaluating the video quality (expected distortion) at the encoder, we also take into account error concealment, which is employed at the decoder to recover packet loss by utilizing the spatial and temporal correlations of video sequences. Note that the scheme of cross-layer resource allocation can also be interpreted as cross-layer error control, from the point of view of error control.

With regard to related work, joint error resilient source coding (quantization parameter and mode selection) and power management for energy efficient wireless video transmission has been studied in [9], premised on a perfect channel coding mechanism. In [10], the selection of source coding parameters is jointly considered with transmitter power and rate adaptation, and packet transmission scheduling for energy efficient wireless video streaming. A joint source coding and power control approach is presented in [11] for optimally allocating source coding rate and bit energy normalized with respect to the multiple-access interference noise density in the context of 3G CDMA networks. The work in [11] did not address error resilient source coding and channel coding. Joint source-channel coding and transmission power allocation has been studied in [12] for progressive image transmission. A joint FEC and transmission power allocation scheme for layered video transmission over a multiple user CDMA network is proposed in [13] based on the 3D-SPIHT codec. Source coding and error concealment are not considered in that work. Joint source-channel coding and processing power control for transmitting layered video

over a 3G wireless network is studied in [14]. An adaptive cross-layer protection scheme is presented in [5] for robust scalable video transmission over 802.11 wireless LANs, where application-layer FEC, the MAC (media access control) retransmission limit, and packet sizes are jointly considered. The work of jointly designing inter-packet and intra-packet FEC for image transmission has been studied in [15] and [16].

In this paper, different from the work mentioned above, we present a joint source-channel coding and power adaptation (JSCCPA) framework for real-time video transmission over an IP-based hybrid wireless/wire-line networks. Specifically, the JSCCPA framework aims to minimize the total end-to-end distortion subject to the resource constraints, which are transmission delay and battery energy in this work. To tackle the resulting optimization problem with two constraints, an efficient algorithm based on Lagrangian relaxation is proposed.

The rest of this paper is organized as follows. We first present some preliminaries in Sect. II. Next, in Sect. III, product FEC and the corresponding packetization are addressed. In Sect. IV, the problem formulation of JSCCPA is presented, followed by the proposed solution algorithm in Sect. V. Experimental results are discussed in Sect. VI. Finally, Sect. VII contains our conclusions.

II. Preliminaries

A. Video Transmission over IP-based Wireless Networks

In a real-time video transmission system over an IP-based wireless network, video packets (referred to as *source packets*) are first generated by a video encoder. In the application layer, the source packets can be re-packetized into *intermediate packets* (e.g., for the purpose of interleaving or FEC). Parity check packets used for FEC may also be generated in this layer if applicable. After passing through the network protocol stack (e.g., RTP/UDP/IP), *transport packets* are formed. Transport packets are transferred to the radio link control (RLC) frames and further to the MAC frames in the link layer in the emerging 3G and 4G systems, such as CDMA2000; these allow both RLC frame retransmissions and MAC frame retransmissions [17]. The current WLAN standard IEEE 802.11 also allows MAC frame retransmission [5]. In this work, in order to make the optimiza-

tion tractable, we assume those retransmissions are disabled. Alternatively, we rely on the link-layer FEC to provide protection, where parity bits are added within packets to further protect against channel bit errors (e.g., CRC is used to provide error check). In this work, like IEEE 802.11, we assume that packets failing that CRC check are rejected at the link layer and thus not forwarded to the IP layer [18]. Therefore, some transport packets may be dropped in the network (due to congestion) or at the receiver (due to unrecoverable bit corruption). For real-time applications, packets arriving at the receiver later than the scheduled playback time are also discarded. Lost packets may be concealed at the decoder.

B. Channel Model

We consider an IP-based hybrid wireless network that consists of both wired and wireless links. In addition to the wired link, the wireless channel can be viewed as a packet erasure channel, as "seen" by the application layer, since packets with errors are not passed from the link layer to the multimedia application [18]. For this reason, as in [19], at the IP level, the network can be modeled as the combination of two independent packet erasure channels: the wired part with loss rate α_k and the wireless part with loss rate β_k. Thus, the overall loss probability of transport packet k in the network is equal to

$$\epsilon_k = \alpha_k + (1 - \alpha_k)\beta_k. \tag{1}$$

In the wired part of the network, packet losses are primarily due to congestion and buffer overflow. These losses can be modeled in various ways, e.g., a Bernoulli process, a 2-state or k-th order Markov chain, etc [20]. In our simulations, we employ a Bernoulli process, i.e., each packet is independently lost with probability α.

In wireless links, we only consider packet losses due to unrecoverable bit errors. Usually, in wireless channels, packets are protected by adding channel bits within packets in the link layer. A packet will be treated as lost if the corrupted bits in this packet cannot all be recovered. Let p_b be the bit error rate (BER) after link-layer channel decoding, i.e., p_b is the BER as seen by the application. Assuming independent bit errors, the loss probability for transport packet k in the wireless channel can be calculated as

$$\beta_k = 1 - (1 - p_b)^{B_{s,k}}, \tag{2}$$

where $B_{s,k}$ is the number of source bits in this transport packet. The BER after channel decoding p_b is a function of the BER before channel decoding, p_e, which is dependent on the state of the radio link, the specific channel code chosen, and the transmission power used. The details of the channel code are addressed in the next subsection. We next discuss how to calculate p_e.

In this work, we consider a flat and fast Rayleigh fading channel plus an Additive White Gaussian Noise (AWGN) process. Note that in this case, the assumption of independent bit errors means that the additive noise and fading are each i.i.d. (independent identically distributed) and independent of each other. If we consider uncoded Binary Phase Shift Keying (BPSK) modulation and assume ideal interleaving, p_e is given by

$$p_e = \frac{1}{2}(1 - \sqrt{\frac{aE_b}{N_0 + aE_b}}), \tag{3}$$

where E_b is the bit energy, N_0 the noise power spectrum density, and a the expected value of the square of the Rayleigh distributed channel gain. [21]. Bit energy is decided by the transmitter power P and the transmission rate R_T for a given modulation scheme. In using BPSK modulation, it can be simply written as $E_b = P/R_T$.

Instead of the above example, the following formulation will also apply to any other channel model for which we can derive a stochastic model of the packet loss probability.

C. End-to-End Distortion

Due to channel losses, we use the expected end-to-end distortion to evaluate video quality. Three factors can be identified as effecting the end-to-end distortion: the source behavior (quantization and packetization), the channel characteristics, and the receiver behavior (error concealment) [1, 2, 22, 23]. The expected distortion can be calculated at the encoder as

$$E[D_k] = (1 - \rho_k)E[D_{R,k}] + \rho_k E[D_{L,k}], \tag{4}$$

where $E[D_{R,k}]$ and $E[D_{L,k}]$ are, respectively, the expected distortion when the k-th source packet is either received correctly or lost, and ρ_k is its loss probability. Note that both $D_{L,k}$ and $D_{R,k}$ are usually random variables. This is because the reference frames for inter-frame coding at the decoder and the encoder may not be the same due to channel losses.

The relationship between the source packet loss probability ρ_k and transport packet loss probability ϵ_k depends on the specific transport packetization scheme chosen. The details of this relationship are discussed in Sect. III.

The calculation of $D_{L,k}$ depends on the specific error concealment strategy used at the decoder. In this work, we consider a simple but efficient temporal concealment scheme: a lost MB is concealed using the median motion vector of its received neighboring MBs (the top-left, top, and top-right). If the previous packet is also lost, then the MB in the same spatial location in the previously reconstructed frame is used to conceal the current loss. For this concealment scheme, the expected distortion for the k-th packet can be written as

$$E[D_k] = (1 - \rho_k)E[D_{R,k}] + \rho_k(1 - \rho_{k-1})E[D_{C,k}] + \rho_k\rho_{k-1}E[D_{Z,k}], \qquad (5)$$

where $E[D_{C,k}]$ and $E[D_{Z,k}]$ are the expected distortions after concealment when packet $k-1$ is either received correctly or lost, respectively. The distortion measurement is based on a per-pixel distortion calculation, which ensures accurate estimation of the end-to-end distortion [22, 24]. Assuming the mean squared error (MSE) criterion, the distortion measurement based on an algorithm called ROPE (Recursive Optimal Per-pixel Estimate) [22] is used to recursively calculate the overall expected distortion level of each pixel.

III. Product Code FEC

The type of FEC used depends on the requirements of the application and the nature of the channel. As mentioned above, packet loss in an IP-based hybrid wireless/wireline network typically has two components: packet loss due to congestion in the wired channel and unrecoverable bit errors due to fading in the wireless channel [18, 19]. One way to combat these two types of packet loss is to use both inter-packet and intra-packet protection. To protect against packet loss in the wired link, inter-packet FEC is performed at the transport layer by generating parity packets in addition to source packets. This is usually achieved by using erasure codes. In the link layer, redundant bits are added within a packet to perform intra-packet protection from bit errors in the wireless link [25]. The combination of the above two techniques, i.e., intra and inter-packet FEC, is termed as product code FEC (PFEC). A PFEC scheme is proposed in [15] to combat

channel variations in progressive image transmission. In that work, intra-packet FEC is achieved through a concatenated CRC/RCPC code, and inter-packet FEC through a systematic Reed-Solomon (RS) code. In [16], an efficient algorithm is provided for finding an optimal equal error protection (EEP) solution for packetized progressive image transmission. Our work considers the use of PFEC in video coding and transmission. An important contribution here is the consideration of UEP for video packets in using PFEC.

A. Forward Error Correction

The most commonly studied erasure codes are based on RS codes, which have good erasure correcting properties and are widely used in practice [4, 5, 12, 16]. Another class of erasure codes that have recently been considered for network applications are Tornado codes, which have slightly worse erasure protecting properties, but can be encoded and decoded much more efficiently than RS codes [26]. In this work, we consider systematic RS codes, but the basic framework could easily be applied to other codes.

An RS code is represented as $RS(n, m)$, where m is the number of source symbols and $(n - m)$ is the number of parity symbols. An RS code can be used to correct both errors and erasures, where an erasure occurs with the position of an error symbol available. The code rate of an $RS(n, m)$ code is defined as m/n. The protection capability of an RS code depends on the block size and the code rate. A limiting factor is the extra delay introduced by the FEC, and therefore the block length, n, is usually determined based on the end-to-end system delay constraints. An $RS(n, m)$ decoder can correct up to $(n - m)/2$ errors or up to $(n - m)$ erasures, regardless of which symbols are lost. The channel errors in the wired link are typically in the form of packet erasures, so an $RS(n, m)$ code applied across packets can correct up to $(n - m)$ lost packets. Thus, with Bernoulli packet losses, the block failure probability (i.e., the probability that at least one of the original m packets is in error) is

$$P_b(n, m) = \sum_{j=n-m+1}^{n} P(n, j) = \sum_{j=n-m+1}^{n} \binom{n}{j} \epsilon^j (1 - \epsilon)^{n-j},$$

where ϵ is the probability of packet loss before error recovery and $P(n, j)$ represents the probability of j errors out of n transmissions.

For performing link-layer FEC, we consider the use of rate-compatible punctured con-

volutional (RCPC) codes [25]. They are adopted in the level 3 of H.223 and H.324 annex C (mobile multiplexer), as part of the mobile version of H.324 [27]. RCPC codes were first introduced in [28]. A family of RCPC codes is described by the mother code of rate $1/N$ and memory M with generator tap matrix of dimension N by $(M+1)$. Together with N, the puncturing period G determines the range of code rates as $R = G/(G+l)$, where l can vary between 1 and $(N-1)G$. The RCPC codes are punctured codes of the mother code with puncturing matrices $\boldsymbol{a}(l) = (a_{ij}(l))$ (of dimension $N \times G$) with $a_{ij}(l) \in (0,1)$, where 0 denotes puncturing.

The decoding of convolutional codes is most commonly achieved using the Viterbi algorithm, which is a maximum-likelihood sequence estimation algorithm. The Viterbi upper bound for the bit error probability is $p_b \leq \frac{1}{G} \sum_{d=d_{free}}^{\infty} c_d p_d$, where d_{free} is the free distance of the convolutional code, p_d is the probability that the wrong path at distance d is selected, and c_d is the number of paths at Hamming distance d from the all-zero path. d_{free} and c_d are parameters of the convolutional code, while p_d depends on the type of decoding (soft or hard) and the channel. The theoretical bounds of BER for RCPC codes can be found in [28, 29]. In this work, we use the simulated BER. The methods for simulation can be found in [28, 29]. We use RCPC codes to perform link-layer FEC, but the proposed framework could easily be applied to other codes as well.

B. Packetization

In the product FEC scheme considered here, the first step is to perform RS coding at the transport layer. As shown in Fig. 1(a), we assume that the source bits in each transport packet correspond to one GOB (group of blocks)[1] and every packet is independently decoded. One GOB is directly packetized into one transport packet by the attachment of a transport packet header. Since the source packet sizes $B_{s,k}$ [shown by the shaded area in Fig. 1(a)] are usually different, the maximum packet size of a block (a group of packets protected by one RS code) is determined first, and then all packets are padded with stuffing bits in the tail part to make the sizes equal. The stuffing bits are removed after the parity packets are generated. Each source packet in Fig. 1(a) is protected by an RS(N, M) code.

---

[1]As in the H.263+ standard [30], we use GOB to denote one row of blocks in the following text.

At the link layer, each packet (including the parity packets) is padded with parity bits. As shown in Fig. 1(b), by using a particular RCPC code with rate r_k, the length of packet k is then $B_k = B_{s,k} + B_{c,k} = B_{s,k}/r_k$.
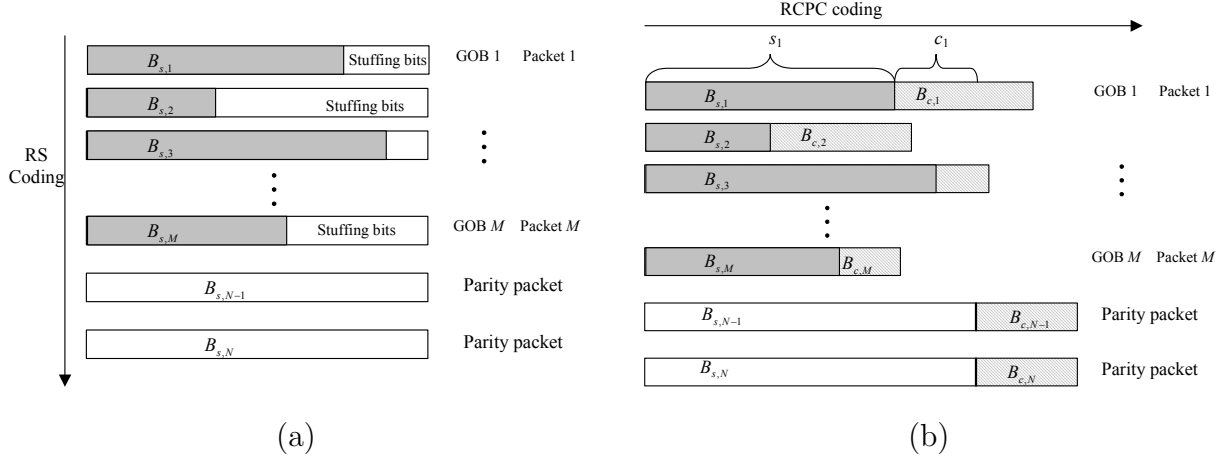

Fig. 1. (a) Step 1: Transport-layer RS coding; (b) Step 2: Link-layer RCPC coding.

Next, we discuss how to calculate the probability of loss for each source packet. Let $\mathcal{Q}$, Γ, $\mathcal{R}$, and $\mathcal{P}$ be the sets of allowable source coding parameters, RS coding parameter, RCPC coding parameters, and transmission power levels, respectively. Let $\mu_k \in \mathcal{Q}$, $\gamma \in \Gamma$, $\nu_k \in \mathcal{R}$, and $\eta_k \in \mathcal{P}$ represent the corresponding parameters selected for the k-th packet. Following the same notation used in [16], let $Q_j^t(N), j = 1, ..., N, t = 1, ..., \binom{N}{j}$ denote the t-th subset with j elements of $Q(N) = \{1, ..., N\}$, and $\overline{Q_j^t}$ its complement. For example, if $N = 3$, then $Q(3) = \{1, 2, 3\}$, $Q_1^1(3) = \{1\}$, $Q_1^2(3) = \{2\}$, $Q_1^3(3) = \{3\}$, $Q_2^1(3) = \{1, 2\}$, $Q_2^2(3) = \{1, 3\}$, $Q_2^3(3) = \{2, 3\}$, $Q_3^1(3) = \{1, 2, 3\}$. Let $I_j(N, k) = \{Q_j^t \subseteq Q(N) | k \in Q_j^t(N), |Q_j^t| = j\}$, then the loss probability of a source packet can be written as

$$
\begin{aligned}
\rho_k(\boldsymbol{\mu}, \gamma, \boldsymbol{\nu}, \boldsymbol{\eta}) &= \sum_{j=N(\gamma)-M+1}^{N(\gamma)} P_{loss,k}(N(\gamma), j) \\
&= \sum_{j=N-M+1}^{N} \sum_{Q_j^t \in I_j(N,k)} \left(\prod_{i \in Q_j^t} \epsilon_i \prod_{l \in \overline{Q_j^t}} (1 - \epsilon_l) \right),
\end{aligned}
\tag{6}
$$

where $P_{loss,k}(N, j)$ is the probability that the k-th packet is not correctly decoded by the RCPC decoder and the total number of transport packets that are not correctly received from the group of N packets is j. Let $\boldsymbol{\mu} = \{\mu_1, \mu_2, ..., \mu_M\}$ denote the vector of source cod-

ing parameters for the M source packets, and $\boldsymbol{\nu} = \{\nu_1, \nu_2, ..., \nu_N\}$ and $\boldsymbol{\eta} = \{\eta_1, \eta_2, ..., \eta_N\}$ the vectors of RCPC coding rates and power levels for the N transport packets in a frame, respectively. Note that the calculation of $\rho_k(\boldsymbol{\mu}, \gamma, \boldsymbol{\nu}, \boldsymbol{\eta})$ itself is rather complicated, as shown in (6). In addition, ρ_k not only depends on the source coding parameter, intra-packet FEC parameter, and power level parameter selected for that packet, but also on the parameters chosen for all the other packets in the frame. This complicated inter-packet dependency stems from two factors. The first complication is due to the fact that the loss probability of a transport packet $\epsilon_k(\mu_k, \nu_k, \eta_k) = \alpha + (1 - \alpha)\beta_k(\mu_k, \nu_k, \eta_k)$ differs from packet to packet[2]. The second complication is due to the inter-packet dependency introduced by inter-packet FEC. Together, these make the expected distortion for one packet depend on the parameters selected for all the packets in the same frame.

IV. Problem Formulation

We first consider real-time video transmission from a mobile device to a receiver through a heterogeneous wireless network. In this case, the efficient utilization of transmission energy is a critical design consideration [31]. In addition, each video packet should meet a delay constraint in order to reach the receiver in time for playback. In an energy-efficient wireless video transmission system, transmission power needs to be balanced against delay to achieve the best video quality [32]. Specifically, for a given transmission rate, increasing the transmission power will increase the energy per bit and consequently decrease BER, as shown in (3), resulting in a smaller probability of packet loss. On the other hand, for a fixed transmission power, increasing the transmission rate will increase the BER but decrease the transmission delay needed for a given amount of data (or allow more data to be sent within a given time-period). Therefore, in order to efficiently utilize resources such as energy and bandwidth, those two adaptation components should be jointly designed.

By jointly considering error resilient source coding $\boldsymbol{\mu}$, transport-layer FEC γ, link-layer FEC $\boldsymbol{\nu}$, power adaptation $\boldsymbol{\eta}$, and error concealment, the JSCCPA problem is formulated

---

[2]As shown in (2), the loss probability for a transport packet in the wireless channel $\beta_k(\mu_k, \nu_k, \eta_k)$ is a function of the source coding parameter, the link-layer FEC parameter, and the transmission power level selected for this packet [since p_b is a function of the channel BER p_e and the link-layer channel rate r_k, where p_e is calculated from (3)].

as:

$$\min_{\{\boldsymbol{\mu}\in\mathcal{Q},\gamma\in\Gamma,\boldsymbol{\nu}\in\mathcal{R},\boldsymbol{\eta}\in\mathcal{P}\}} E[D] = \sum_{k=1}^{M} E[D_k(\boldsymbol{\mu},\gamma,\boldsymbol{\nu},\boldsymbol{\eta})]$$

$$\text{s.t.} \quad C = \sum_{k=1}^{N(\gamma)} B_k P_k(\eta_k)/R_T \leq C_0 \tag{7}$$

$$T = \sum_{k=1}^{N(\gamma)} B_k/R_T \leq T_0,$$

where B_k and P_k are, respectively, the number of bits (including both source bits and channel bits) and the power level for the k-th packet; M and N are, respectively, the number of source packets and the total number of transport packets in one frame; R_T is the transmission rate; and C_0 and T_0 are the energy and transmission delay constraint for the frame, respectively.

As a special case, we also focus on the last hop of a wireless network and consider transmitting real-time video from a mobile device to the base station over a single wireless link; this is likely to be the bottleneck of the whole video transmission system. In Sect. VI-B, we show through simulations that inter-packet FEC is not helpful in this case (at least for the cases we have simulated). Thus, in this special case, we do not use transport-layer FEC. By jointly considering error resilient source coding, link-layer FEC, and power adaptation, we formulate a JSCCPA problem given below for video transmission over a wireless link,

$$\min_{\{\boldsymbol{\mu}\in\mathcal{Q},\boldsymbol{\nu}\in\mathcal{R},\boldsymbol{\eta}\in\mathcal{P}\}} E[D] = \sum_{k=1}^{M} E[D_k(\boldsymbol{\mu},\boldsymbol{\nu},\boldsymbol{\eta})]$$

$$\text{s.t.} \quad C = \sum_{k=1}^{M} B_k(\mu_k,\nu_k) P_k(\eta_k)/R_T \leq C_0 \tag{8}$$

$$T = \sum_{k=1}^{M} B_k(\mu_k,\nu_k)/R_T \leq T_0.$$

Note that in this case, we have $\rho_k(\mu_k,\nu_k,\eta_k) = \beta_k(\mu_k,\nu_k,\eta_k)$, which means that the probability of loss for one packet depends only on the parameters selected for this packet. Consequently, the expected distortion for one packet depends only on the parameters selected for this packet and its previous packet, based on (5).

V. Solution Algorithm

In this section, we present solutions for (7) and (8) based on Lagrangian relaxation. Depending on the complexities of the inter-packet dependencies, the resulting two minimization problems can be efficiently solved using an iterative descent algorithm that is based on the method of alternating variables for multivariate minimization [33] and deterministic dynamic programming, respectively.

A. Lagrangian Relaxation

First, we formulate a Lagrangian dual for (7) by introducing Lagrange multipliers, $\lambda_1 \geq 0$ and $\lambda_2 \geq 0$, for the transmission energy and delay constraints, respectively. The resulting Lagrangian is

$$L(\boldsymbol{\mu}, \gamma, \boldsymbol{\nu}, \boldsymbol{\eta}, \lambda_1, \lambda_2) = E[D] + \lambda_1(C - C_0) + \lambda_2(T - T_0) \tag{9}$$

and the corresponding dual function is

$$g(\lambda_1, \lambda_2) = \min_{\{\boldsymbol{\mu} \in \mathcal{Q}, \gamma \in \Gamma, \boldsymbol{\nu} \in \mathcal{R}, \boldsymbol{\eta} \in \mathcal{P}\}} L(\boldsymbol{\mu}, \gamma, \boldsymbol{\nu}, \boldsymbol{\eta}, \lambda_1, \lambda_2). \tag{10}$$

Note that the Lagrangian may not be separable because the distortion for the k-th packet, $E[D_k]$, may depend on the parameters chosen for the other packets. The dual problem to (7) is then given by

$$\max_{\lambda_1 \geq 0, \lambda_2 \geq 0} g(\lambda_1, \lambda_2). \tag{11}$$

Solving (11) will provide a solution to (7) within a convex hull approximation. Assuming we can evaluate the dual function for a given choice of λ_1 and λ_2, a solution to (11) can be found by choosing the correct Lagrange multipliers. This can be accomplished by using a variety of methods such as cutting-plane or sub-gradient methods [34]. Alternatively, based on the observed structure of this problem, we propose the following heuristic approach, which is considerably more efficient than the above-mentioned methods.

Figure 2 illustrates four possible cases of the energy contour $C = C_0$ and the delay contour $T = T_0$ in the $\lambda_1 - \lambda_2$ plane, where C_0 and T_0 are the transmission energy and transmission delay constraints for one frame, respectively. The shaded area indicates the valid choices of (λ_1, λ_2) that satisfy both constraints. The triangle point in each figure
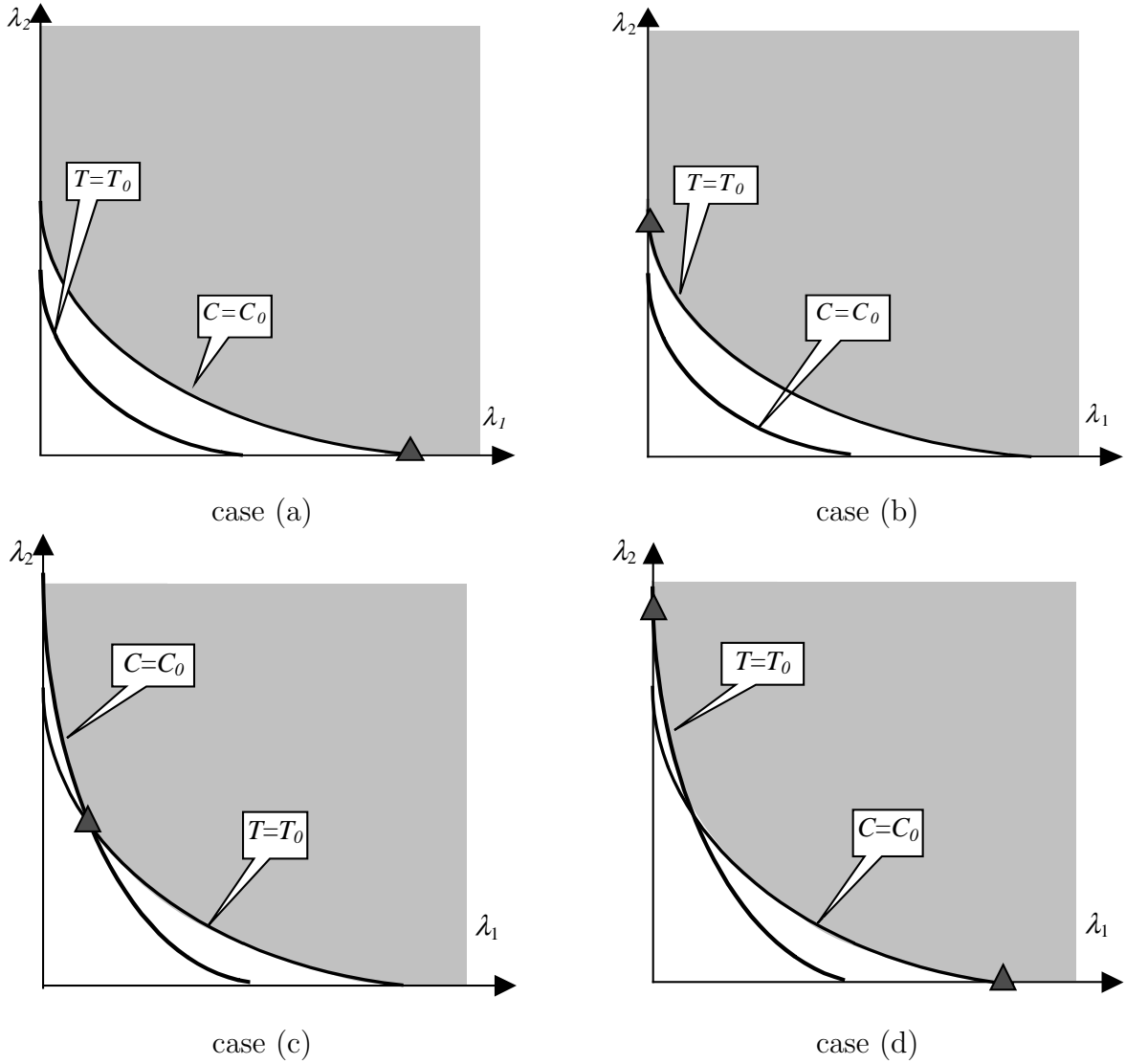
Fig. 2. Four cases of cost and delay contours.

represents the location of the optimal solution. To derive our heuristic, let us assume that this problem has no duality gap. In this case, from complementary slackness, the optimal solution must lie at one of the points where the contours intersect the axis or at the intersection of the contours[3]. In Fig. 2, we show the contours intersecting at only one point; this is the only case we have observed in practice, and we assume that it is true in the following. Let $H \in \mathcal{Q} \times \Gamma \times \mathcal{R} \times \mathcal{P}$, then the appropriate (λ_1, λ_2) can be obtained using the algorithm described below.

[3]If we consider the convex hull of the primal problem (i.e. we take the convex hull of the constraint set); then if Slater's condition is satisfied, this problem will have no duality gap.

Step 1 (*case a, d*): Let $\lambda_2 = 0$, find the largest λ_1^* such that $C(H(\lambda_1^*, 0)) \le C_0$. If $T(H(\lambda_1^*, 0)) \le T_0$, $H(\lambda_1^*, 0)$ is the solution. Otherwise,

Step 2 (*case b, d*): Let $\lambda_1 = 0$, find the largest λ_2^* such that $T(H(0, \lambda_2^*)) \le T_0$. If $C(H(0, \lambda_2^*)) \le C_0$, $H(0, \lambda_2^*)$ is the solution. Otherwise,

Step 3 (*case c*):

i. Let $\lambda_1^l = 0$, $\lambda_1^r = \lambda_1^*$, $\lambda_2^b = 0$, $\lambda_2^t = \lambda_2^*$ (where λ_1^* and λ_2^* are given in steps 1 and 2).

ii. Let $\lambda_1^m = (\lambda_1^l + \lambda_1^r)/2$, find λ_2^* within $[\lambda_2^b, \lambda_2^t]$ to satisfy $T(H(\lambda_1^m, \lambda_2^*)) \le T_0$.

iii. If $C(H(\lambda_1^m, \lambda_2^*)) > C_0$, then let $\lambda_1^l = \lambda_1^m$, $\lambda_2^t = \lambda_2^*$, and go to step 3ii. Otherwise,

iv. If $C(H(\lambda_1^m, \lambda_2^*)) < C_0 - \delta$ (δ is a relatively small number), then let $\lambda_1^r = \lambda_1^m$, $\lambda_2^b = \lambda_2^*$, and go to step 3ii. Otherwise,

v. Let the solution be $H(\lambda_1^m, \lambda_2^*)$.

In the proposed solution, when one Lagrange multiplier is fixed, the dual problem becomes a one-dimensional problem, which can be easily solved by standard convex search techniques, such as the bisection method [35]. Note that in cases (a) and (b), one of the constraints is inactive. Case (d) indicates that different combinations of (λ_1, λ_2) may result in the same minimum distortion. Next, we consider evaluating the dual function in (10), given appropriate λ_1 and λ_2.

B. Minimization of Lagrangian

In (7), for given Lagrange multipliers, minimizing the resulting Lagrangian itself is still complicated due to the fact that the loss probability of one source packet depends on the operational parameters chosen for all the other packets. Hence, we solve the minimization problem by an iterative descent algorithm that is based on the method of alternating variables for multivariate minimization [33]. To be precise, for each RS code $\gamma \in \Gamma$ (i.e., we do an exhaustive search for γ), the RS block size is $N(\gamma)$, which is also the number of total transport packets in a frame. Then by adjusting one set of operational parameters for one packet at a time, while keeping constant those for the other packets until convergence, we can minimize the Lagrangian, $L(\boldsymbol{\mu}, \gamma, \boldsymbol{\nu}, \boldsymbol{\eta}, \lambda_1, \lambda_2)$ in (9). In particular, let $x_k = \{\mu_k, \nu_k, \eta_k\}$ denote the vector of the source coding, intra-FEC channel coding, and power level selected for the k-th packet, and $\boldsymbol{x} = \{x_1, x_2, ..., x_N\}$ denote the

parameters selected for the N packets[4]. Let $\boldsymbol{x}^{(t)} = \{x_1^{(t)}, x_2^{(t)}, ..., x_N^{(t)}\}$, for $t = 0, 1, 2, ...$, be the parameter vector selected by optimization at step t, where $\boldsymbol{x}^{(0)}$ corresponds to any initial parameter vector selected for the N packets. This can be done in a round-robin style, e.g., let $t_n = (t \mod N)$. If $i \neq t_n$, let $x_i^{(n)} = x_i^{(n-1)}$. Otherwise, for $i = t_n$, the following optimization is carried out

$$x_i^{(t)} = arg \min_{\boldsymbol{x}^{(t)}} L(x_1^{(t)}, ..., x_{i-1}^{(t)}, x_i, x_{i+1}^{(t)}, ..., x_N^{(t)}, \lambda_1, \lambda_2). \tag{12}$$

The optimal operational parameter vector $\boldsymbol{x}^{(t)}$ is updated until the Lagrangian $L(\boldsymbol{x}^{(t)}, \gamma,$ $\lambda_1, \lambda_2)$ converges. Convergence is guaranteed because the Lagrangian is non-increasing and bounded below [13]. In fact, in our simulations, we have observed that it only takes two to three iterations for the Lagrangian to converge. The computational complexity mainly comes from the calculation of (6), which depends on the block size of the RS code, $N(\gamma)$. Note that the above iterative algorithm generates a set of optimal parameters of $(\boldsymbol{\mu}, \boldsymbol{\nu}, \boldsymbol{\eta})$ for a particular γ. The final optimal parameters $(\boldsymbol{\mu}, \gamma, \boldsymbol{\nu}, \boldsymbol{\eta})$ corresponds to the minimum Lagrangian with one particular γ and its corresponding optimal parameters of $(\boldsymbol{\mu}, \boldsymbol{\nu}, \boldsymbol{\eta})$.

If the special case, i.e., formulation (8), is considered, we can accurately (since the global optimal solution is guaranteed) and efficiently minimize the resulting Lagrangian by using DP due to the limited inter-packet dependencies[5]. For simplicity, let C_k and T_k denote the transmission energy and transmission delay for packet k, respectively. The Lagrangian corresponding to formulation (8) can be expressed as $L(\boldsymbol{\mu}, \boldsymbol{\nu}, \boldsymbol{\eta}, \lambda_1, \lambda_2) = \sum_{k=1}^{M} J(k)$, where

$$J(k) = E[D_k] + \lambda_1 C_k + \lambda_2 T_k.$$

From (2) and (4), the cost of each packet $J(k)$ is a function of μ_k, ν_k, η_k and $E[D_{L,k}]$. As shown in (5), if we employ the error concealment strategy described in Sect. II-C, the cost of the k-th packet can be described as

$$J(k) = J(\mu_{k-1}, \nu_{k-1}, \eta_{k-1}, \mu_k, \nu_k, \eta_k).$$

[4]Note that for $k > M$, there is no associated source coding parameter μ_k defined, because these packets are parity packets. However, the number of source bits in those parity packets is determined by the maximum of the source bits in the source packets.

[5]Note that due to the use of inter-packet FEC in (7), where the expected distortion for one packet depends on the parameters selected for all the packets in the same frame, DP is not applicable in (7).

The dual can then be evaluated via dynamic programming. The time complexity[6] of this scheme is $O(M \cdot |\mathcal{Q} \times \mathcal{R} \times \mathcal{P}|^2)$ [35]. Note that if a simpler error concealment scheme is used, i.e., the lost MB is recovered from the MB with the same spatial location in the previously reconstructed frame, the cost for packet k is in the form of

$$J(k) = J(\mu_k, \nu_k, \eta_k),$$

resulting in a time complexity of $O(M \cdot |\mathcal{Q} \times \mathcal{R} \times \mathcal{P}|)$.

VI. Experimental Results

A. Implementation Issues

In our simulations, we choose an H.263+ codec [30] to perform source coding. We use an RCPC code with generator polynomials (133, 171), mother code rate 1/2, and puncturing rate $G = 4$. This mother rate is punctured to achieve the 4/7, 2/3, and 4/5 rate codes. At the receiver, soft Viterbi decoding is used in conjunction with BPSK demodulation. We present experiments on flat and fast Rayleigh fading channels, and the channel parameter is defined as $\text{SNR} = a\frac{E_b}{N_0}$, where a is the expected value of the square of the channel gain due to Rayleigh fading. In the simulations, the bit error rates for the Rayleigh fading with the assumption of ideal interleaving were obtained experimentally using simulations, as shown in Table I. The test sequence used in the reported experiments is the QCIF (176×144) Foreman sequence at a frame rate of 30 fps. Similar results are also obtained using other test sequences such as Akiyo, Container, and Coastguard.

The distortion measurement is based on the ROPE algorithm [22]. To clearly illustrate the proposed JSCCPA framework, we assume that channel feedback is available to the encoder in the form of which packets are received or lost. Feedback is only utilized in the calculation of the expected distortion and limits the impact of error propagation. In all experiments, the feedback delay is set as 4 frames (133.3 milliseconds). We emphasize that the feedback delay is long enough to preclude retransmissions in this setting. Rate control is not implemented in this work. Thus, every frame has the same transmission delay constraint of one frame time. The image quality measure used is the peak signal-to-

---

[6]Note that here we only discuss the time complexity for evaluating the dual given particular Lagrange multipliers. The total time complexity depends on the number of times needed to find the correct Lagrange multipliers.

noise ratio (PSNR), defined by PSNR= $10 \log \frac{255^2}{\text{MSE}}$ dB. Note that the PSNR values shown in all the plots below are the average decoded PSNR averaged over 50 random channel error realizations under each setting.

Channel SNR (dB)	2	6	10	14	18	22
Channel rate=1/2	1.4×10^{-3}	2.2×10^{-5}	2.1×10^{-6}	2.4×10^{-7}	6.4×10^{-8}	2.8×10^{-9}
Channel rate=4/7	1.1×10^{-1}	5.3×10^{-4}	4.1×10^{-5}	1.1×10^{-5}	3.8×10^{-6}	1.3×10^{-6}
Channel rate=2/3	3.2×10^{-1}	7.4×10^{-3}	1.7×10^{-4}	3.5×10^{-5}	1.2×10^{-5}	4.2×10^{-6}
Channel rate=4/5	4.2×10^{-1}	4.0×10^{-2}	6.6×10^{-4}	1.1×10^{-4}	3.6×10^{-5}	1.2×10^{-5}

TABLE I

PERFORMANCE OF RCPC OVER A RAYLEIGH FADING CHANNEL WITH INTERLEAVING.

B. Video Transmission over Hybrid Wireless Networks

We first evaluate the performance of the proposed PFEC on a hybrid wireless network, which consists of both wired and wireless links. We fix the transmission power in this study. This is mainly due to the high computation complexity in calculating (7) if all those operational components are included. In addition, this simplified case allows us to better analyze the potential of the proposed PFEC approach in providing UEP. For the transport-layer inter-packet FEC, we choose $\Gamma = \{(9,9), (11,9), (13,9), (16,9)\}$ as the available RS coding set. Longer blocks not only complicate the computation of (6), but also introduce longer delays. The transmission rate is set as $R_T = 360$ kbps in all simulations of this subsection.

B.1 Product FEC vs. Link-Layer FEC

In this experiment, we compare the performances of two UEP systems: i) the UEP product code FEC (UPE-PFEC) and ii) pure link-layer FEC (UEP-LFEC). The goal is to illustrate the advantage of using PFEC. Both systems are UEP optimized using (7), where the PFEC system allows transport-layer RS coding but the LFEC system does not. The two systems have the same energy and transmission delay constraints.

We illustrate the performance of the two systems in Fig. 3, where we plot the average decoded PSNR for various average SNR values in the wireless link and packet loss rates

α in the wired link. As shown in Fig. 3, with the above simulation setup, when α is small, LFEC is close to PFEC. However, as the wired link gets worse, PFEC starts to outperform LFEC by up to 2.5 dB. This improved performance is due to the use of cross-packet protection in the transport layer. Table II shows how link-layer FEC rates are selected in the two systems. As can be seen, as the channel SNR improves, less link-layer protection is needed, i.e., higher channel rates are used. Second, compared to the LFEC approach, the PFEC approach uses lower rate codes of link-layer FEC because of the overhead from the transport-layer FEC. In addition, we can see in the table that the link-layer FEC rates do not follow the change of α. This implies that the link-layer FEC is apparently less efficient than transport-layer FEC in reacting to packet losses in the wired link, because the link-layer FEC does not provide inter-packet protection. Another observation from Fig. 3(a) is that when $\alpha = 0$, which corresponds to the case where the wired link is error free, the inter-packet FEC in the transport layer becomes unnecessary and thus the optimized PFEC is equivalent to LFEC.
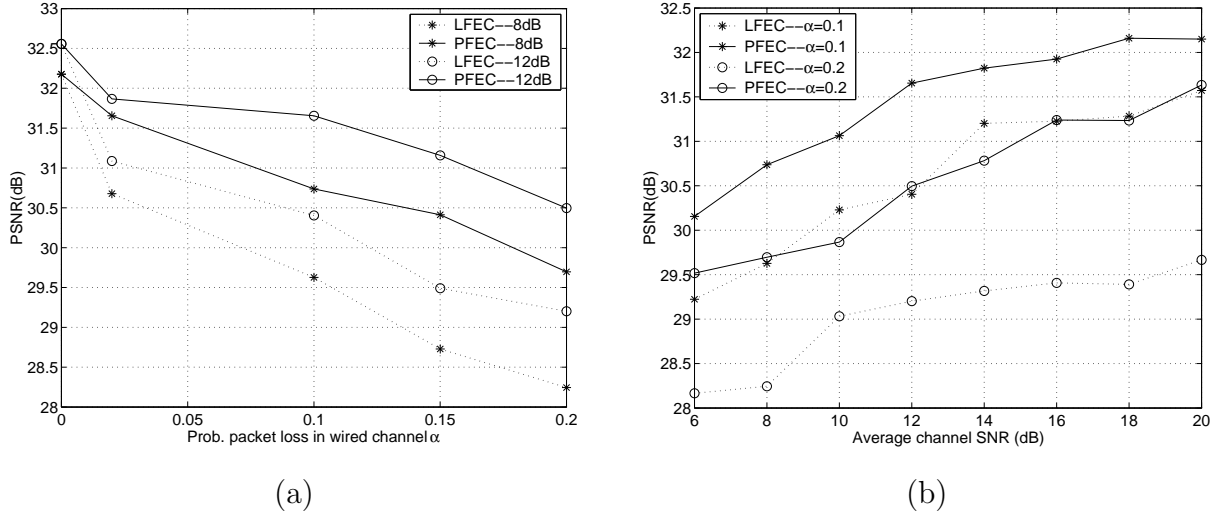

Fig. 3.   (a) PSNR vs. α (b) PSNR vs. average channel SNR, for PFEC and LFEC.

B.2 UEP vs. EEP

In the second experiment, we illustrate the advantage of UEP by comparing the performance of two PFEC systems: i) UEP product FEC (UEP-PFEC) and ii) EEP product FEC (EEP-PFEC). Both systems use a product FEC and are optimized within (7). The

α	Channel SNR (dB)	Link-layer FEC rates in percentage in UEP-PFEC				Link-layer FEC rates in percentage in UEP-LFEC			
		cr=1/2	cr=4/7	cr=2/3	cr=4/5	cr=1/2	cr=4/7	cr=2/3	cr=4/5
	6	28.9	68.9	0.7	1.5	94.8	5.2	0	0
	8	26.7	5.2	68.1	0	63	8.9	28.1	0
0.1	10	3	0	89.6	7.4	28.9	0	71.1	0
	12	0.7	0	80.8	18.5	7.4	0	91.1	1.5
	16	0.7	0	23.7	75.6	0	0	80	20
	6	54.1	45.9	0	0	91.1	8.9	0	0
	8	17.8	10.4	71.8	0	47.4	11.9	40.7	0
0.2	10	2.2	0	97.8	0	23.7	0	76.3	0
	12	2	0	98	0	3	0	94	3
	16	1.5	0	11.8	86.7	0	0	60	40

TABLE II

LINK-LAYER FEC RATES IN PERCENTAGE IN THE UEP-PFEC AND UEP-LFEC SYSTEM (CR
DENOTES CHANNEL RATE).

difference is that the EEP system has fixed link layer FEC, while the link layer FEC in
the UEP system is optimally employed. For the two systems, we plot in Fig. 4 the aver-
age decoded PSNR under different average channel SNR. It can be seen that UEP-PFEC
achieves the upper bound of all EEP-PFEC systems, and outperforms the best of all EEP
systems by around 0.2 dB at all channel conditions. The gain comes from the higher
flexibility of the UEP-PFEC approach, where link-layer coding parameters can be opti-
mally assigned to different packets to achieve UEP for video packets that are of different
importance.

C. Video Transmission over Wireless Links

In this study, we consider video transmission over a single wireless link. This can be
regarded as a special case of hybrid wireless networks where the wired link is error and
delay free. In the study above, we have shown that when the wired link has no errors
($\alpha = 0$), transport-layer inter-packet FEC is not necessary; thus it is omitted, which
makes the computations much more efficient. The goal of this subsection is to study the
effectiveness of channel coding (intra-packet FEC) and power adaptation in achieving the
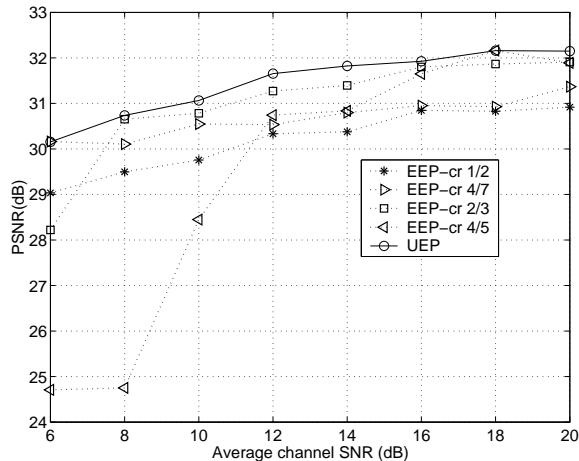
Fig. 4. PSNR vs. average channel SNR (α=0.1), for UEP and EEP.

optimal UEP. We focus on the trade-off of the two adaptation components.

C.1 Performance Comparison of JSCPA and RERSC Systems

In this experiment, we compare the performance of two systems: the proposed framework in (8) with fixed channel coding rate, which is referred to as JSCPA (joint source coding and power adaptation) system, and an RERSC (reference error resilient source coding) system which uses a fixed channel coding rate and transmission power. The transmission power levels can be adapted depending on the CSI and source content in the JSCPA system, but is fixed in the RERSC system. We refer to the RERSC system as the reference system, and evaluate it under different channel SNR (referred to as reference channel SNR) to generate the energy constraints for the JSCPA system. Thus, the two systems have the same transmission delay constraints and use the same amount of transmission energy.

We illustrate the performance of the two systems in Fig. 5(a), which shows the average decoded PSNR for the Foreman sequence under different channel SNR when $R_T = 360$ kbps, and Fig. 5(b), where we plot the average decoded PSNR versus transmission rate when the reference channel SNR is 12 dB. As shown in Fig. 5, by adjusting the power levels, the JSCPA system achieves a significant gain over the RERSC system. When the channel SNR is small, e.g., 8 dB, the gain can be as large as 6 dB in PSNR. The gain comes from the higher flexibility of the JSCPA approach, where the power level can

be optimally assigned to different packets to achieve UEP for video packets that are of different importance. In addition, from Fig. 5, we can see that under some settings, JSCPA achieves little gain over RERSC [e.g., when the channel SNR is 12 dB and the channel coding rate used is low, as shown in Fig. 5(b)]. This observation can help us assess the effective components in designing a practical video streaming system. Table III shows how transmission power is optimally selected for transmitting video packets in the proposed JSCPA system. The values inside the parentheses denote the percentage of packets with transmission power level 1, 2, 3, 4, 5, respectively. Note that the power level parameters 1, 2, 3, 4 and 5 are simplified substitutes for the actual transmission power values. The actual values are proportional to those parameters.

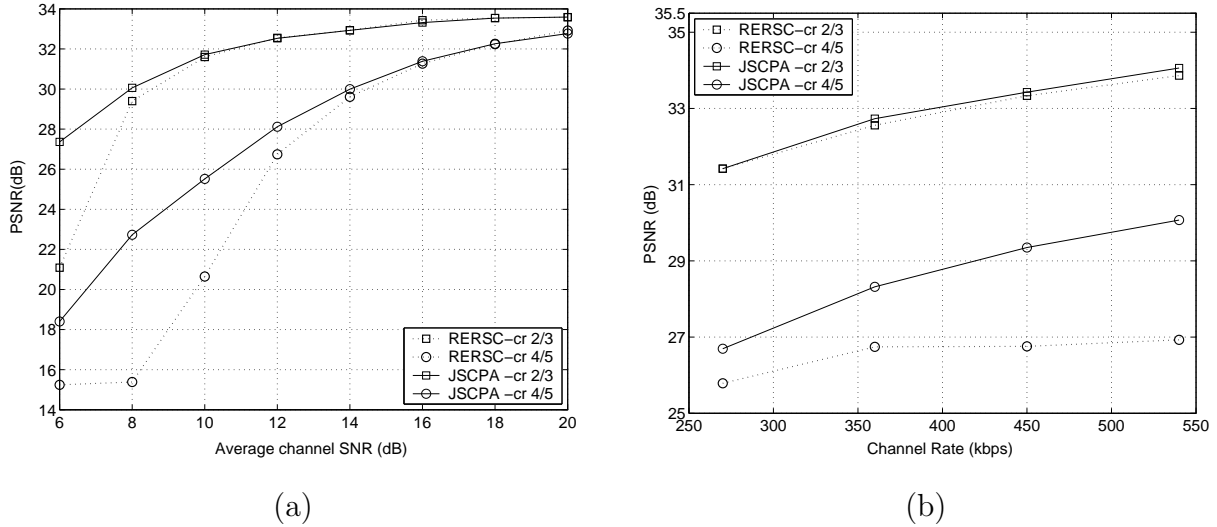(a)   (b)

Fig. 5.   JSCPA vs. RERSC (a) PSNR vs. average channel SNR with $R_T = 360$ kbps (b) PSNR vs. transmission rate with reference channel SNR be 12 dB (cr denotes channel rate in the legend).

C.2 Performance Comparison of JSCCPA and JSCPA Systems

In the second experiment, we compare the performance of the JSCCPA system as in (7) and the JSCPA (joint source coding and power adaptation) system, in which the channel coding parameter is fixed. Note that the two systems have the same transmission delay and energy constraints, which are obtained from the corresponding reference RERSC systems. For the two systems, we plot the average decoded PSNR for the Foreman sequence under different channel SNRs when $R_T = 360$ kbps in Fig. 6(a) and at different transmission

Reference SNR (dB)	6	12	20
Channel rate=1/2	(2.4,18.5,73.9,5.1,0)	(12.6,32.4,33.9,19.6,1.4)	(62.3,0,12.9,0,24.8)
Channel rate=4/7	(18,0,14.3,66.1,1.6)	(2.3,29.9,56.4,11.0,0.3)	(10,35,39.2,13.4,2.3)
Channel rate=2/3	(40,0,0,13,47)	(0.7,13.9,66.1,18.7.0.6)	(11.6,10.8,69.1,6.9,1.6)
Channel rate=4/5	(45.8,0,0,0,54.2)	(2,4.1,41.8,47.3,4.9)	(8.2,31.5,43.8,15.3,1.3)

TABLE III

POWER LEVEL ALLOCATION OF POWER LEVEL $(1,2,3,4,5)$ IN PERCENTAGE IN THE JSCPA SYSTEM

(THE REFERENCE POWER LEVEL IS 3).

rates when the reference channel SNR is 12 dB in Fig. 6(b). It can be seen that the JSCCPA approach achieves the upper bound of all JSCPA approaches. The gain comes from the higher flexibility of the JSCCPA approach, where channel coding parameters can be optimally assigned to different packets to achieve UEP. Table IV shows how channel coding rates are selected by the JSCCPA system. As can be seen, as the channel SNR improves, less channel protection is needed.
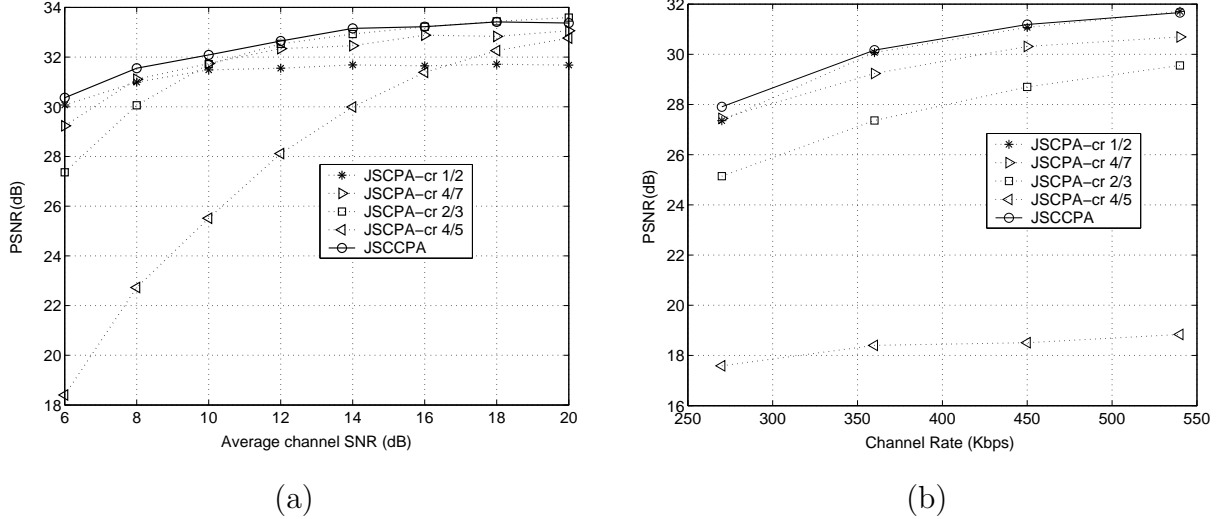

(a)   (b)

Fig. 6.   JSCCPA vs. JSCPA (a)PSNR vs. average channel SNR with $R_T = 360$ kbps (b) PSNR vs. channel transmission rate with the reference channel SNR be 12 dB (cr denotes channel rate in the legend).

Reference SNR (dB)	6	8	10	12	14	16	18	20
Channel rate=1/2	96.2	67.7	41.2	19.6	6.7	4.7	1.0	1.6
Channel rate=4/7	3.8	31.9	57.3	69.6	61.3	35.0	17.8	5.6
Channel rate=2/3	0	0.4	1.5	10.8	31.3	57.7	73.9	69.6
Channel rate=4/5	0	0	0	0	0.7	2.6	7.3	23.2

TABLE IV

CHANNEL CODING RATES IN PERCENTAGE IN JSCCPA SYSTEM.

VII. CONCLUSIONS

We have studied cross-layer resource allocation for energy efficient video communications over a hybrid wireless/wire-line network. By assuming that the encoder can access and specify the resource allocation parameters in the underlying layers, the cross-layer resources are optimally allocated according to the joint source-channel coding and power adaptation (JSCCPA) framework, where various error control components, such as error resilient source coding, transport-layer FEC, link-layer FEC, power adaptation and error concealment, are jointly considered. Our focus is on the channel coding and power adaptation.

We first demonstrated the outstanding performance of the proposed PFEC which can provide optimal UEP for video streams. Next, through simulations on a hybrid wireless network, we showed that transport-layer FEC is not necessary if the wired link has no error, based on our simulation setups. In addition, we demonstrated the advantage of jointly adapting the link-layer FEC and transmission power to the varying wireless channel conditions.

The proposed framework not only provides an optimization benchmark against which the performances of other sub-optimal systems can be evaluated, but also gives rise to a useful tool in assessing the effectiveness of different adaptation components in practical system design. In addition, the proposed algorithm based on Lagrangian relaxation can be generally used to tackle the optimization problem with two constraints.

References

[1] F. Zhai, Y. Eisenberg, T. N. Pappas, R. Berry, and A. K. Katsaggelos, "Joint source-channel coding and power allocation for energy efficient wireless video communications," in *Proc. 41st Allerton Conf. Communications, Control, and Computing*, Oct. 2003.

[2] F. Zhai, Y. Eisenberg, T. N. Pappas, R. Berry, and A. K. Katsaggelos, "Rate-distortion optimized product code forward error correction for video transmission over IP-based wireless networks," in *Proc. IEEE Int. Conf. Acoustics, Speech, and Signal Processing ICASSP'04)*, Montreal, Quebec, Canada, May 2004, to appear.

[3] H. Zheng, "Optimizing wireless multimedia transmissions through cross layer design," in *Proc. IEEE*, Baltimore, MD, July 2003, vol. 1, pp. 185–188.

[4] F. Zhai, Y. Eisenberg, T. N. Pappas, R. Berry, and A. K. Katsaggelos, "Rate-distortion optimzied hybrid error control for real-time packetized video transmission," in *Proceedings of ICC'04*, Paris, French, June 2004.

[5] M. var der Schaar, S. Krishnamachari, S. Choi, and X. Xu, "Adaptive cross-layer protection strategies for robust scalable video transmission over 802.11 WLANs," *IEEE J. Select. Areas Commun.*, vol. 21, pp. 1752–1763, Dec. 2003.

[6] L. Hanzo, "Bandwidth-efficient wireless multimedia communications," *Proc. IEEE*, vol. 86, no. 7, pp. 1342–1998, July 1998.

[7] Z. Fu, X. Meng, and S. Lu, "A transport protocol for supporting multimedia streaming in mobile ad hoc networks," *IEEE J. Select. Areas Commun.*, vol. 21, pp. 1615–1626, Dec. 2003.

[8] S. Blake, D. Black, M. Carlson, E. Davies, Z. Wang, and W. Weiss, "An architecture for differentiated services," Tech. Rep., RFC 2475, IETF, Dec. 1998, http://www.rfc-editor.org/rfc/rfc2475.txt.

[9] Y. Eisenberg, C. E. Luna, T. N. Pappas, R. Berry, and A. K. Katsaggelos, "Joint source coding and transmission power management for energy efficient wireless video communications," *IEEE Trans. on Circuits and System for Video Technology*, vol. 12, no. 6, pp. 411–424, June 2002.

[10] C. E. Luna, Y. Eisenberg, R. Berry, T. N. Pappas, and A. K. Katsaggelos, "Joint source coding and data rate adaptation for energy efficient wireless video streaming," *IEEE J. Select. Areas Commun.*, vol. 21, pp. 1710–1720, Dec. 2003.

[11] Y. S. Chan and J. W. Modestino, "A joint source coding-power control approach for video transmission over CDMA networks," *IEEE J. Select. Areas Commun.*, vol. 21, pp. 1516–1525, Dec. 2003.

[12] S. Appadwedula, D. L. Jones, K. Ramchandan, and L. Qian, "Joint source channel matching for wireless image transmission," in *Proc. IEEE Int. Conf. Image Processing*, Chicago, IL, Oct. 1998.

[13] S. Zhao, Z. Xiong, and X. Wang, "Joint error control and power allocation for video transmission over CDMA networks with multiuser detection," *IEEE Trans. Circ. and Syst. for Video Techn.*, vol. 12, pp. 425–437, June 2002.

[14] Q. Zhang, W. Zhu, and Y.-Q. Zhang, "Network-adaptive scalable video streaming over 3G wireless network," in *Proc. IEEE Int.Conf. Image Processing*, Thessaloniki, Greece, Oct. 2001.

[15] P. G. Sherwood and K. Zeger, "Error protection for progressive image transmission over memoryless and fading channels," *IEEE Trans. Comm.*, vol. 46, pp. 1555–1559, Dec. 1998.

[16] V. Stanković, R. Hamzaoui, and Z. Xiong, "Product code error protection of packetized multimedia bit-streams," in *Proc. IEEE ICIP*, Barcelona, Spain, Sept. 2003.

[17] P. Luukkanen, Z. Rong, and L. Ma, "Performance of 1XTREME system for mixed voice and data communications," in *Proceedings IEEE Inf. Conf. Communications*, Helsinki, Finland, June 2001, pp. 1411–1415.

[18] D. A. Eckhardt, *An Internet-style approach to managing wireless link errors*, Ph.D Thesis, Carnegie Mellon University, Pittsburgh, PA, May 2002.

[19] G. Cheung, W.-T. Tan, and T. Yoshimura, "Rate-distortion optimized application-level retransmission using streaming agent for video streaming over 3G wireless network," in *Proceedings IEEE Inf. Conf. Image Processing*, Rochester, New York, Sept. 2002.

[20] M. Yajnik, S. Moon, J. Jurose, and et al., "Measurement and modeling of the temporal dependence in packet loss," Tech. Rep. 98-78, UMASS CMPSCI, 1998.

[21] T. S. Rappaport, *Wireless communications principle and practice*, Prentice Hall, 1998.

[22] R. Zhang, S. L. Regunathan, and K. Rose, "Video coding with optimal inter/intra-mode switching for packet loss resilience," *IEEE J. Select. Areas Commun.*, vol. 18, pp. 966–976, June 2000.

[23] D. Wu, Y. T. Hou, B. Li, W. Zhu, Y.-Q. Zhang, and H. J. Chao, "An end-to-end approach for optimal mode selection in Internet video communication: theory and application," *IEEE J. Select. Areas Commun.*, vol. 18, no. 6, pp. 977–995, June 2000.

[24] R. O. Hinds, T. N. Pappas, and J. S. Lim, "Joint block-based video source-channel coding for packet-switched networks," *Proc. SPIE*, vol. 3309, pp. 124–133, Jan. 1998.

[25] N. Celandroni and F. Pototì, "Maximizing single connection TCP goodput by trading bandwidth for BER," *Int. J. of Commun. Syst.*, vol. 16, pp. 63–79, Feb. 2003.

[26] A. Albanese, J. Blomer, J. Edmonds, M. Luby, and M. Sudan, "Priority encoding transmission," *IEEE Trans. Inform. Theory*, vol. 42, pp. 1737–1744, Nov. 1996.

[27] *Multiplexing protocol for low bitrate multimedia communication over highly error-prone channels*, ITU-T Draft of H.223 Annex C, Sept. 1997.

[28] J. Hagenauer, "Rate-compatible punctured convolutional codes (RCPC codes) and their applications," *IEEE Trans. Commun.*, vol. 36, pp. 389–400, Apr. 1988.

[29] J. G. Proakis, *Digital Communications*, McGraw-Hill, New York, Aug. 2000.

[30] ITU-T, *Video coding for low bitrate communication*, ITU-T Recommendation H.263, Jan. 1998, Version 2.

[31] N. Bambos, "Toward power-sensitive network architectures in wireless communications: Concepts, issues, and design aspects," *IEEE J. Select. Areas commun.*, vol. 18, pp. 966–976, June 2000.

[32] C. E. Luna, *Video Quality and Network Efficiency Trade-Offs in Video Streaming Applications*, Ph.D Thesis, Northwestern University, Evanston, IL, June 2002.

[33] R. Fletcher, *Practical methods of optimization*, New York: Wiley, 2nd edition, 1987.

[34] D. Bertsekas, *Nonlinear Programming*, Athena Scientific, Belmont, MA, 1995.

[35] G. M. Schuster and A. K. Katsaggelos, *Rate-Distortion Based Video Compression: Optimal Video Frame Compression and Object Boundary Encoding*, Kluwer Academic Publishers, 1997.